J. Micromech. Microeng. **10** (2000) 528–533. Printed in the UK PII: S0960-1317(00)13844-6

A capacitive absolute-pressure sensor with external pick-off electrodes

J-S Park† and Y B Gianchandani‡§

† Department of Mechanical Engineering, University of Wisconsin, Madison, WI 53706-1691, USA
‡ Department of Electrical and Computer Engineering, 1415 Engineering Drive, University of Wisconsin, Madison, WI 53706-1691, USA

E-mail: yogesh@engr.wisc.edu

Received 10 May 2000, in final form 14 July 2000

Abstract. This paper describes a capacitive absolute-pressure sensor in which the sealed lead transfer is eliminated. The pick-off capacitance is between a flap or skirt-like extension of the flexible diaphragm that reaches past the sealed cavity, and an electrode patterned on the substrate directly below this extension. The sidewall of the cavity is relatively narrow and flexible. Finite-element analysis is used to explore the relevance of various dimensional parameters and to estimate the sensitivity and temperature coefficients of the device. The device is fabricated from p^{++} Si on a glass substrate using the dissolved wafer process with three masking steps. The measurements of fabricated devices with 1 mm radius, 7 μm cavity height, and 8 μm wall thickness show -84 ppm kPa^{-1} sensitivity at room temperature in touch-mode operation. In non-touch-mode operation the sensitivity is significantly higher. A reference device with similar dimensions shows a less than 22 ppm K^{-1} temperature coefficient of offset below 150 °C.

1. Introduction

Capacitive pressure sensors are attractive for many applications because they offer relatively high sensitivity, low power consumption, and small temperature coefficients [1]. The traditional approach in microfabricating these devices has been to read the capacitance between a flexible conductive diaphragm and an electrode located directly beneath it. The cavity between the diaphragm and the electrode is sealed under vacuum to provide absolute-pressure sensing capability and to eliminate the deleterious effects of expansion or contraction of trapped gases. Unfortunately, this gives rise to the problem of how to transfer the electrode lead from the sealed cavity to the exterior, where it can be accessed by interface electronics. Various solutions have been developed in the past. In one approach, a hole is etched or drilled in the substrate or in a rigid portion of the microstructure next to the flexible diaphragm, the lead is transferred through it, and then it is sealed with epoxy or metals [2, 3]. In another approach, lithographically patterned subsurface feed-throughs planarized by chemical–mechanical polishing are used to transfer the lead [4]. In a third approach, the cavity of the pressure sensor is formed by undercutting a deposited layer on the front side of the substrate wafer. The opening in this layer, which provides access for the etchant, is subsequently sealed under vacuum by another deposited thin film [5, 6]. In contrast, this paper describes a new design for sealed capacitive pressure sensors by which the sealed lead transfer is eliminated, allowing the devices to be fabricated with very few photolithography steps [7]. The devices are fabricated using a standard processing technique that has been used for a variety of micromachined sensors in the past. The design permits moderate sensitivity and a wide dynamic range. The performance can be easily tailored to various application regimes by adjusting the dimensional parameters.

§ Author to whom correspondence should be addressed.

2. Device structure and modeling

The new pressure sensors eliminate the problem of sealed lead transfer by locating the pick-off capacitance outside the sealed cavity, as illustrated in figure 1. A skirt extends outward from the periphery of the vacuum-sealed cavity, acting as the electrode that deflects under pressure. The stationary electrode is a thin-film metal layer patterned on the substrate below this skirt. As the external pressure increases, the center of the diaphragm deflects downwards, and the periphery of the skirt rises, reducing the pick-off capacitance. This deflection continues monotonically as the external pressure increases beyond the value at which the center of the diaphragm touches the substrate, so this device can be operated in the touch mode for an expanded dynamic range [8]. In figure 1, $T1$ is the thickness of the skirt or flap; $T2$ is the thickness of the sidewalls; $T3$ is the thickness

0960-1317/00/040528+06$30.00

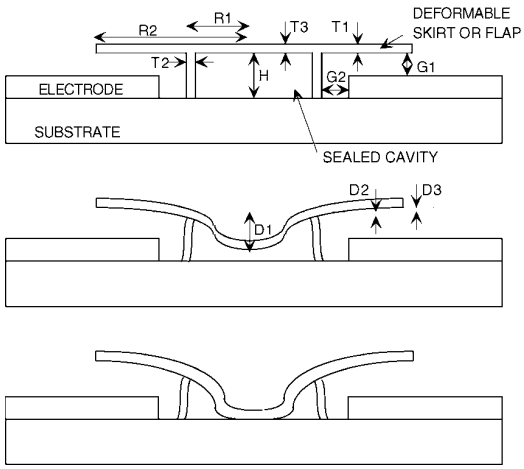

Figure 1. Structure of the capacitive pressure sensor at equilibrium, with the external pressure equal to sealed cavity pressure (top), in non-touch-mode operation (middle), and touch-mode operation (bottom). In the touch mode, the diaphragm area in contact with the substrate increases as the external pressure increases.

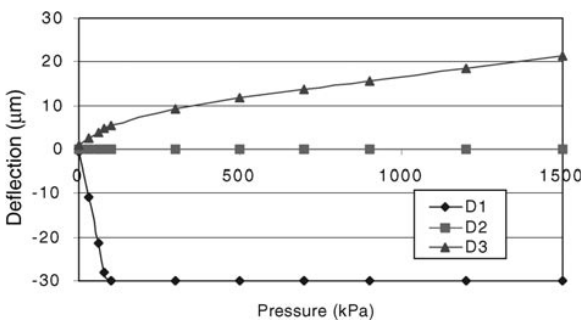

Figure 2. The deflection at the center ($D1$), support points ($D2$), and periphery ($D3$) of a diaphragm as a function of the pressure across the diaphragm. The device dimensions are $T1 = T2 = T3 = 5\ \mu$m, $R1 = 500\ \mu$m, $R2 = 1000\ \mu$m, $H = 30\ \mu$m, and $G1 = 5\ \mu$m.

of the cap over the sealed cavity, which may potentially be bossed; $R1$ is the radius of the sealed cavity; $R2$ is the radius of the device; H is the height of the sealed cavity; $G1$ is the nominal gap between the skirt and the electrode; $G2$ is the clearance between the electrode and sidewalls; $D1$ is the deflection at the center of the diaphragm; $D2$ is the deflection at the sidewall support; and $D3$ is the deflection at the skirt perimeter.

Although the geometry of the proposed device is simple, its response to applied pressure is not conveniently expressed by a closed-form analytical expression because all three elements of its structure, including the inner diaphragm, the outer skirt, and the sidewalls, flex in response to an applied pressure. For example, the deflection at the outer edge of the skirt is only about 15% of what would be present if the diaphragm was simply supported at the cylinder sidewalls. Consequently, nonlinear finite-element analysis (FEA) has been used to predict the device response. The deflection was analyzed in ANSYS^{TM}, using Solid72 element (which provides a suitable compromise between the accuracy and the execution time) for the structural material, and Contac52 for the gap. The material properties were consistent with

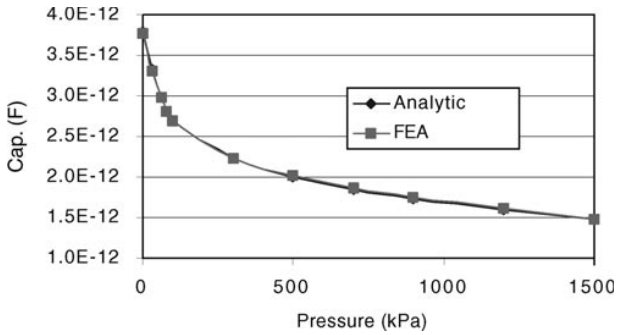

Figure 3. Sense capacitance as a function of pressure across the diaphragm, obtained by electrostatic FEA and analytical formula. The sensitivities are -2900 ppm kPa^{-1} (-11.2 fF kPa^{-1}) and -270 ppm kPa^{-1} (-0.52 fF kPa^{-1}) in the non-touch and touch modes, respectively.

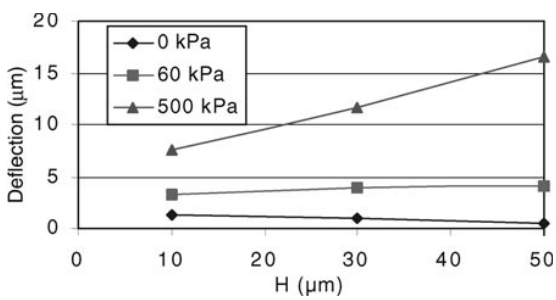

Figure 4. The effect of the cavity height (H) on deflection $D3$ at the perimeter. The device dimensions are as in figure 2.

the intended fabrication process, which uses p^{++} Si for the diaphragm and Corning^{TM} 7740 glass for the substrate [9]. This process results in a tensile residual stress of +20 MPa in the diaphragm, which was included in the simulations. In order to reduce computation time, a 10° axisymmetric section of the pressure sensor was analyzed.

The FEA results for a device with $T1 = T2 = T3 = 5\ \mu$m, $R1 = 500\ \mu$m, $R2 = 1000\ \mu$m, $H = 30\ \mu$m, and $G1 = 5\ \mu$m are shown in figure 2. As the external pressure is increased, the center of the diaphragm rapidly descends, hitting the bottom very close to atmospheric pressure. Thereon the device operates in touch mode, and the contact area between the diaphragm and substrate continues to increase with applied pressure. The outer edge of the skirt rises monotonically at a rate of about 0.05 μm kPa^{-1} in the non-touch mode and 0.011 μm kPa^{-1} in the touch mode.

The pick-off capacitance as a function of the deflection skirt can be calculated analytically using the formula

$$C = 2\pi\varepsilon_0 \int_{R1}^{R2} \frac{r\,\mathrm{d}r}{G1 + (r - R1)\tan\phi} \qquad (1)$$

where ϕ is the angle made by the skirt to the substrate. The output capacitance can also be found by FEA using electrostatic modeling. Both analytical and FEA results for the capacitance changes corresponding to the deflections plotted in figure 2 have been obtained, and are in close agreement (figure 3). The sensitivity of this device is then determined as -2900 ppm kPa^{-1} (-11.2 fF kPa^{-1}) in the non-touch mode and -270 ppm kPa^{-1} (-0.52 fF kPa^{-1}) in the touch mode.

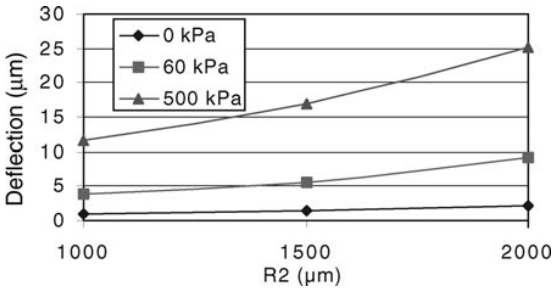

Figure 5. The effect of the perimeter radius ($R2$) on deflection D3 at the perimeter. The device dimensions are as in figure 2.

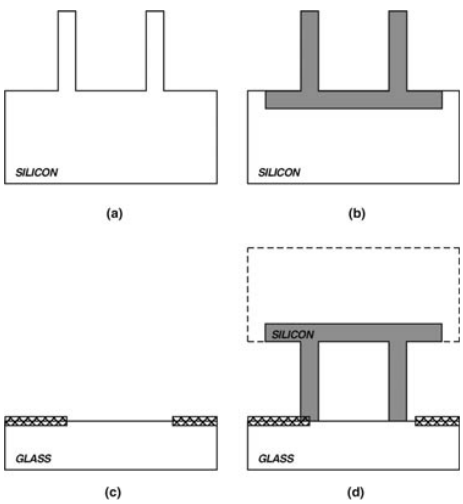

Figure 6. Description of the dissolved wafer process. (a) Etch the profile of the pressure sensor into a silicon substrate wafer using reactive ion etching or any other method (mask 1). (b) Diffuse boron to define the structural thickness. Eventually, the undoped regions will be dissolved away (mask 2). (c) Inlay a glass wafer with metal to form the fixed electrodes for the sense capacitor as well as the interconnect (mask 3). (d) Anodically bond the silicon and glass wafers face to face, and dissolve the undoped silicon in a dopant-selective etchant (no mask).

In exploring the design space using the FEA, it is clear that the overall device sensitivity is very dependent on the height of the sidewalls (H) and the radius of the skirt ($R2$). Figures 4 and 5 show that, at high pressures, $D3$, the deflection of the skirt perimeter, more than doubles as H is increased from 10 to 50 μm, or as $R2$ is increased from 1 to 2 mm.

FEA has also been used to determine temperature coefficients of sensitivity and offset that would exist due to the thermal expansion mismatch between silicon and glass. The temperature coefficient of offset (TCO), which is defined as $\Delta C/(C\Delta T)$, is 80 ppm K^{-1} in the non-touch mode. The temperature coefficient of sensitivity (TCS), which is defined as $S\Delta S/(S\Delta T)$ where S represents sensitivity, is 77 and 31 ppm K^{-1} in the non-touch and touch modes, respectively. In this model the expansion coefficient of the silicon was assumed to be 0.1 ppm K^{-1} larger than that of glass. In reality, this value is accurate only at room temperature, and increases with temperature because of the unequal changes in the expansion coefficients of Si and glass [10]. Thus, the TCO and TCS estimates are accurate only in the vicinity of room temperature.

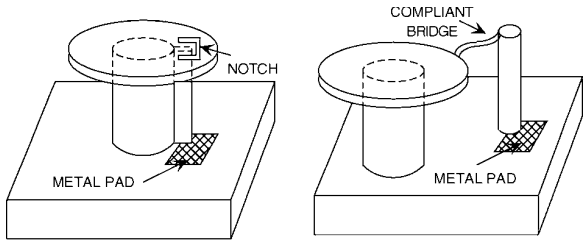

Figure 7. Two options for lead transfer to the diaphragm: a protrusion in the sidewall with an optional notch in the skirt and a compliant bridge to a remote anchor.

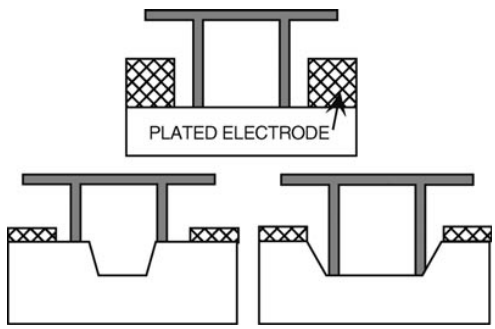

Figure 8. The process options to increase pick-off capacitance: plating up the electrode (upper figure), and recessing the glass (lower figures).

3. Fabrication and measurement results

Although the skirted pressure sensor can be fabricated by a variety of methods, the dissolved wafer process was used for the first implementation because of its simplicity [9]. This three-mask process is illustrated in figure 6. A silicon wafer is first dry etched to the desired height of the cavity and then selectively diffused with boron to define the radius of the pressure sensor. The depth of the boron diffusion determines the eventual thickness of the structural layer. The silicon wafer is then flipped over and anodically bonded to a glass wafer that has been inlaid with a Ti/Pt metal pattern that serves as the interconnect and provides the bond pads. The undoped Si is finally dissolved in ethylene diamine pyrocatechol (EDP), leaving the pressure sensor on the glass substrate. The key challenges in this sequence are the second lithography step and the anodic bonding, in both cases as a result of the high aspect ratio of the cavity sidewalls.

A structural challenge caused by process limitations is how to make electrical contact with the deflecting diaphragm without adversely affecting device performance or manufacturability. The standard approach of overlapping the silicon anchor area with metal lines on the glass substrate is complicated by the narrow anchors necessary to maintain the flexibility of this structure: if misalignment at the bonding step causes the metal to traverse the width of the cavity wall, the hermeticity of the cavity seal will be lost. Two approaches are explored: in one, the lead transfer is made at a protrusion that extends from the sidewall. It has a relatively large footprint, allowing increased alignment tolerance. A notch may be optionally cut in the skirt around it to retain the sensitivity of the device. In the other approach, a complaint air bridge of p^{++} Si extends from the flexible diaphragm to a

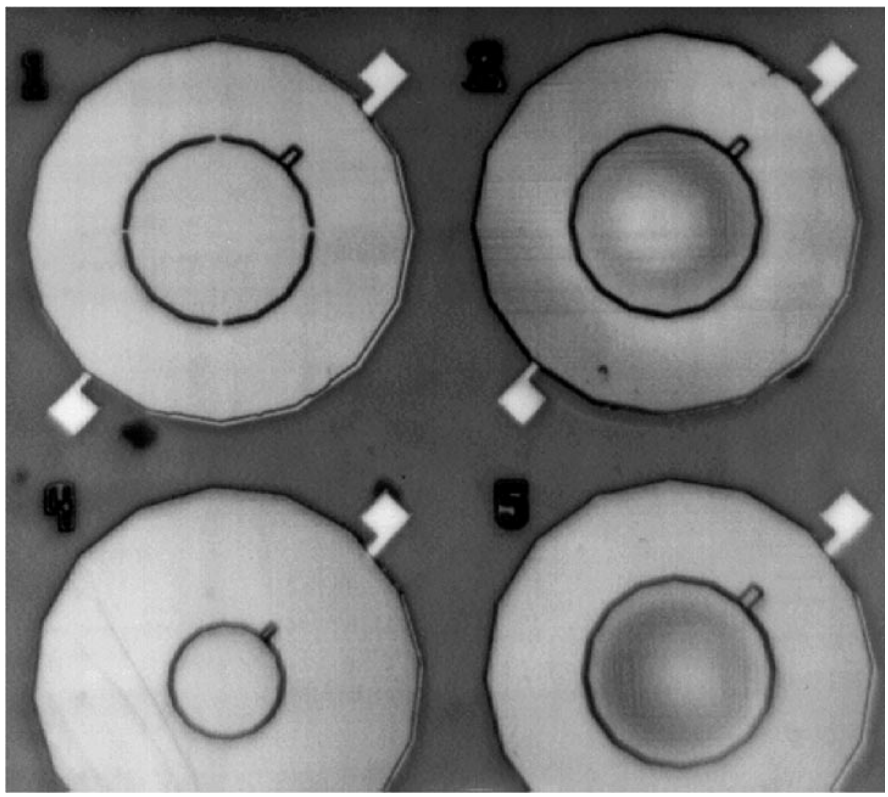

Figure 9. An optical micrograph of a fabricated array of pressure sensors. The device on the top left was designed with breaks in the sidewall to serve as a reference capacitor for process and temperature compensation. The two devices on the right show prominent dimpling above the sealed cavities, indicating the reduced pressure inside.

post which is anchored to the substrate some distance away, where the lead is transferred in the traditional manner. These approaches are illustrated in figure 7.

A potential performance-related concern in the sensor design is the possibility of reduced sense capacitance because of the large gap between the skirt and electrode. Figure 8 illustrates ways to reduce the capacitor gap without changing the shape of the deformable structure; for example by thickening the electrode by electroplating or recessing the glass substrate, which requires upto one additional mask. Sealed capacitive pressure sensors with various dimensions have been designed and fabricated. Figure 9 shows an array of devices with differing $R1$'s and wall widths $T2$. On the top left of the figure is a reference capacitor, designed with breaks in the sidewall for process and temperature compensation. In the top and bottom right-hand-side devices, note the dimple created in the cap above the sealed cavity by the pressure difference between the ambient and the interior. Figure 10 shows scanning electron micrographs of fabricated devices using the lead transfer methods illustrated in figure 7. Note that the groove formed by the boron diffusion profile at the location of the sidewalls is in fact very shallow, although it appears dark in the optical photograph of figure 9.

Preliminary tests have been performed on the fabricated pressure sensors at the wafer level using a probe station. Figure 11 shows the measured pressure response of a device with $R1 = 500\ \mu$m, $R2 = 1000\ \mu$m, $T1 = T2 = T3 = 8\ \mu$m, and $H = 7\ \mu$m. The device was sealed under partial vacuum, with a residual pressure of 25 kPa at room temperature. It was operating in touch mode for the pressure regime in which it was tested, and its measured sensitivity was -84 ppm kPa^{-1} (-0.25 fF kPa^{-1}).

The TCO was measured between 150 and 300 °C using a reference capacitor. The gaps in its sidewall ensure that the pressure across diaphragm is zero. As shown in figure 12, the value at the high end of this temperature range is 1.2 fF K^{-1} (405 ppm K^{-1}), while at the low end it is 0.07 fF K^{-1} (22 ppm K^{-1}). The increase of the TCO with temperature is due to unequal changes in the thermal expansion coefficients of the Si and the glass [10]. The TCO was difficult to measure at temperatures lower than 150 °C because of the resolution limits of the test equipment. The temperature insensitivity of the output is a significant advantage in some applications.

4. Conclusions

Pressure sensors are one of the most commercially viable applications of micromachining technology, and are used in many different arenas such as the automotive, biomedical and industrial instrumentation industries. This paper has presented a device design that is fundamentally different from the existing options in solving the problem of lead transfer in traditional, sealed, capacitive pressure sensors. Extensive FEA indicates that a device with $R1 = 500\ \mu$m, $R2 = 1000\ \mu$m, $T1 = T2 = T3 = 5\ \mu$m, $H = 30\ \mu$m, and $G1 = 5\ \mu$m can provide sensitivity as high as -2900 ppm kPa^{-1} in the non-touch mode and

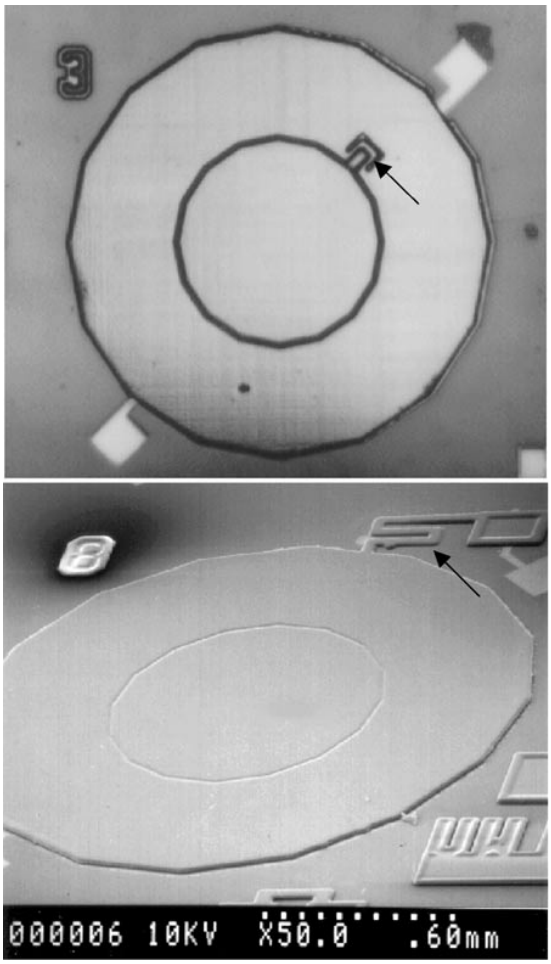

Figure 10. Fabricated devices showing the lead transfer methods illustrated in figure 7: an optical micrograph of the notch method (upper figure), and an SEM image of the compliant bridge method (lower figure).

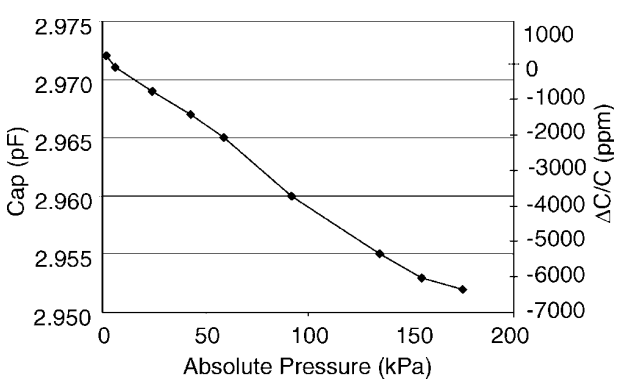

Figure 11. The touch-mode sensitivity of a fabricated pressure sensor with $R1 = 500\ \mu$m, $R2 = 1000\ \mu$m, $T1 = T2 = T3 = 8\ \mu$m, and $H = 7\ \mu$m was about 80 ppm kPa^{-1}. The measurement accuracy was ± 1 fF.

-270 ppm kPa^{-1} in the touch mode, with a TCO of 80 ppm K^{-1} and a TCS of 30–80 ppm K^{-1}. Although the sensitivity is lower than that of conventional capacitive pressure sensors of similar size, it is comparable to that of piezoresistive pressure sensors. The temperature coefficients are relatively very small.

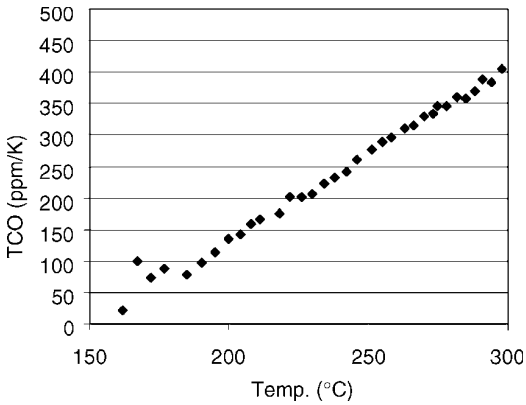

Figure 12. The measured TCO for a reference pressure sensor (designed with gaps in the sidewall). The device dimensions are as in figure 11. Each data point is averaged over three readings.

Pressure sensors were fabricated by a three-mask dissolved wafer process that is well established as a micromachining technique. Methods for increasing the output capacitance and sensitivity were described, and approaches for transferring the signal from the flexible diaphragm to the substrate were developed. Initial tests of the fabricated devices with $R1 = 500\ \mu$m, $R2 = 1000\ \mu$m, $T1 = T2 = T3 = 8\ \mu$m, and $H = 7\ \mu$m, have validated the concept of this pressure sensor. A touch-mode sensitivity of -84 ppm kPa^{-1} was measured at room temperature, and a TCO of 22 ppm K^{-1} was measured below about 150 °C.

Future efforts will focus on the packaging of the fabricated devices. One possible approach is to package the sensors in a chemically-inert dielectric liquid. This will serve to transfer the pressure, keep the capacitor free of particles, and increase the sense capacitance by its dielectric constant.

Acknowledgments

The authors gratefully acknowledge Mr L L Chu for extensive help with testing; Mr A Salian of the University of Michigan, and Mr Koo and Professor N Hershkowitz of the University of Wisconsin Plasma Research Center for help with the reactive ion etching; Professor E Lovell of the University of Wisconsin Mechanical Engineering Department for discussions; and the staff of the Wisconsin Center for Applied Microelectronics for technical support.

References

[1] Lee Y S and Wise K D 1982 A batch-fabricated silicon capacitive pressure transducer with low temperature sensitivity *IEEE Trans. Electron Devices* **29** 42–8

[2] Wang Y and Esashi M 1997 A novel electrostatic servo capacitive vacuum sensor *Proc. IEEE Int. Conf. on Solid-State Sensors and Actuators, Transducers '97 (June 1997)* pp 1457–60

[3] Giachino J M, Haeberle R J and Crow J W 1981 *US Patent Specification* 4261086
Giachino J M, Haeberle R J and Crow J W 1981 *US Patent Specification* 4386453

Peters A J and Marks E A 1986 *US Patent Specification* 4586109

[4] Chavan A V and Wise K D 1997 A batch-processed vacuum-sealed capacitive pressure sensor *Proc. IEEE Int. Conf. on Solid-State Sensors and Actuators (Transducers '97) (June 1997)* pp 1449–52

[5] Guckel H, Burns D W, Rutigliano C R, Showers D K and Uglow J 1997 Fine grained polysilicon and its application to planar pressure transducers *Proc. IEEE Int. Conf. on Solid-State Sensors and Actuators (Transducers '97) (June 1997)* pp 277–82

[6] Sugiyama S, Suzuki T, Kawahata K, Shimaoko K, Takigawa M and Igarashi I 1986 Micro-diaphragm pressure sensor *Tech. Dig., IEEE Int. Conf. on Electron Devices (Los Angeles, CA)* pp 184–7

[7] Park J-S and Gianchandani Y B 1999 A low-cost batch-sealed capacitive pressure sensor *Proc. IEEE Int. Conf. on Micro Electro Mechanical Systems, MEMS '99 (Orlando, FL, January 1999)* pp 82–7

[8] Cho S T, Najafi K, Lowman C E and Wise K D 1992 An ultrasensitive silicon pressure-based microflow sensor *IEEE Trans. Electron Devices* **39** 825–35

[9] Gianchandani Y B and Najafi K 1992 A bulk silicon dissolved wafer process for microelectromechanical devices *IEEE J. Microelectromech. Syst.* **1** 77–85

[10] Ko W H, Suminto J T and Yeh G J 1985 Bonding techniques for microsensors *Micromachining and Micropackaging of Sensors* (Amsterdam: Elsevier)

Ko W H, Suminto J T and Yeh G J 1990 *Microsensors* ed R S Muller *et al* (Piscataway, NJ: IEEE)